



1 Roadway backfill method to prevent geo-hazards induced by room 2 and pillar mining: a case study in Changxing coal mine, China

3 Jixiong Zhang¹, Meng Li¹, Nan Zhou¹, Rui Gao¹

4 ¹Key Laboratory of Deep Coal Resource Mining, School of Mines, Ministry of Education of China, China University of
5 Mining and Technology, Xuzhou 221116, China

6 *Correspondence to:* Meng Li (limeng1989@cumt.edu.cn)

7 *These authors contributed equally to this work and should be considered co-first authors

8 **Abstract.** Coal mines in the western areas of China experience low mining rates and induce many geo-hazards when using
9 the room and pillar mining method. In this research, we proposed a roadway backfill method during longwall mining to
10 target these problems. We tested the mechanical properties of the backfill materials to determine a reasonable ratio of
11 backfill materials for the driving roadway during longwall mining. We also introduced the roadway layout and the backfill
12 mining technique required for this method. Based on the effects of the abutment stress from a single roadway driving task,
13 we designed the distance between roadways and a driving and filling sequence for multiple-roadway driving. By doing so,
14 we found the movement characteristics of the strata with quadratic stabilisation for backfill mining during roadway driving.
15 Based on this research, the driving and filling sequence of the 3101 working face in Changxing coal mine was optimised to
16 avoid the superimposed influence of mining-induced stress. According to the analysis of the surface monitoring data, the
17 accumulated maximum subsidence is 15mm and the maximum horizontal deformation is 0.8 mm/m, which indicated that the
18 ground basically had no obvious deformation after the implementation of the roadway backfill method at 3101 working face.

19 1 Introduction

20 Recently, due to the high intensity and large scale of coal mining around the world, problems associated with resources and
21 the environment have become more severe with each passing day, and many mining induced hazards have been caused (Shi
22 and Singh 2001; Castellanza et al. 2010; Pasten et al. 2015; Zhai et al. 2016). The effects of these problems are especially
23 prominent in the ecologically vulnerable areas of western China (Si et al. 2010; Ding et al. 2014). Many small and medium-
24 sized coal mines in this area use room and pillar mining method (Kostecki and Spearing 2015), and have a mining rate of
25 less than 30%, which leading to abandonment of the coal resources in underground. In addition, the burial depth of the coal
26 seams in the region is usually shallower. During mining, geological behaviour becomes more important, threatening mine
27 production safety and usually causing unpredictable disasters, such as surface subsidence, landslides and water inrush caused
28 by karst environments (White 2002; Parise 2012; Lollino et al. 2013; Parise 2015). In particular, when karst caves are at
29 shallow depth, the effects at the ground surface may be extremely severe (Parise and Lollino 2011), and the direct



30 connection between the surface and the underlying karst aquifers usually function as a channel for water inrush (Gutierrez et
31 al. 2014), thus posing a great threat to coal mines. At present, previous studies proposed strip mining (Chen et al. 2012; Guo
32 et al. 2014a) to resolve these problems. However, strip mining resulted in a low mining rate of coal resources as well as other
33 problems. To resolve these difficulties, this research proposes roadway backfill technique in longwall mining based on the
34 solid backfill mining method (Zhang et al. 2011; Junker and Witthaus 2013; Guo et al. 2014b). This method has been
35 recently developed and has become popular and applied on a large scale, providing an effective solution to the previously
36 mentioned problems.

37 Recently, research into the strip filling method has promoted the development of the roadway filling method and its
38 underlying theory (Zhang et al. 2007; Yu and Wang 2011; Chen et al. 2011; Sun and Wang 2011), but few studies have been
39 conducted on backfilling the driving roadway during longwall mining, especially from the perspective of the strata
40 movement characteristics. Moreover, different types of backfill materials with different mechanical properties exist, and if
41 the room and pillar mining method is adopted, strata behaviour becomes the most important factor at shallow burial depths.
42 Consequently, the characteristics of the strata movement in regions mined using this approach are significantly different
43 from those in traditionally-mined regions. The room and pillar mining method is normally used for shallow mines in western
44 China to prevent the overlying strata from caving in and collapsing. A great quantity of coal resources is abandoned
45 underground due to the use of the room and pillar method, which has caused a huge waste of coal resources. Additionally,
46 the coal pillars creep over time and gradually fail (Bell and Bruyn 1999; Castellanza et al. 2008). During pillar failure, the
47 roof strata become fractured and the collapse progresses upwards (Ghasemi et al. 2012; Cui et al. 2014). Finally, surface
48 subsidence results in building damage, environmental destruction, etc. The Changxing coal mine is used as a case study in
49 this paper, and the roadway backfill method is proposed to solve the problems discussed above. We tested the mechanical
50 properties of a backfill material composed of common aeolian sand, loess, and a cementing material. We also simulated
51 strata movement characteristics with different roadway driving and filling sequences by FLAC^{3D} software. Finally, we used
52 the research results to design the 3101 working face in the Changxing coal mine.

53 **2 Geological and mining conditions**

54 The room and pillar mining method was originally adopted in the Changxing coal mine, resulting in a mining rate of only
55 30%. In addition, problems such as severe surface subsidence and significant coal loss caused by the instability of the mined
56 rooms and coal pillars have threatened the mining field, as shown in Fig. 1. Meanwhile, due to coal pillar failure, magnitude
57 2.5 and 2.8 earthquakes have occurred in the Changxing coal mine, leading to the deterioration of vegetation, water loss and
58 ecological damage. At present, only the integrated coal areas in the 3101, 3103, 3015, and 3107 working faces can be mined
59 in Changxing coal mine. Under these circumstances, roadway backfill method in longwall mining was used to solve these
60 problems. In this method, backfill materials are used to fill the mined-out area, serving as a permanent stress bearing body
61 that supports the overburden. Overlying strata may slowly sink as a consequence, therefore it is of critical importance that



62 strata movement and surface subsidence is effectively controlled. Additionally, the mining rate could be improved to a great
63 degree. The primary mineable coal bed of the mining field was designed as a coal seam with an average thickness, angle, and
64 burial depth of 5.35 m, 0.5 °, and approximately 130 m, respectively. The immediate roof, main roof, and floor are siltstone,
65 fine-sandstone, and carbonaceous mudstone with average thicknesses of 4.5 m, 11.6 m, and 7.6 m, respectively.

66 **3 Testing of the mechanical properties of the backfill material**

67 **3.1 Sample preparation & test scheme**

68 The Changxing coal mine is located in western China, where the surface of the earth is covered by aeolian sand and loess, so
69 we used aeolian sand and loess as the principal backfill materials for maximum cost reduction. To improve its resistance to
70 deformation, the backfill material was comprised of three kinds of material: aeolian sand, loess, and a cementing material.
71 Specifically, aeolian sand and loess were used as a coarse aggregate and a fine aggregate, respectively. After mixing with the
72 cementing material, test samples of the backfill material were prepared. The testing scheme is shown in Table 1. The
73 mechanical properties of each backfill material were a result of triplicate tests on each sample.

74 **3.2 Test instrument**

75 The SANS material testing machine was used and provided a maximum axial force of 300 kN over a cross-head
76 displacement range of 250 mm. The compaction device was a home-made compaction steel chamber containing the backfill
77 material. Its inner diameter was 125 mm and its outer diameter was 137 mm, while its height was 305 mm. The radius and
78 height of the compression piston were 124 mm and 40 mm, respectively (Li et al. 2014). A load was applied by the test
79 machine via a compression piston fitted to the compaction device (see Fig. 2).

80 **3.3 Analysis of test results**

81 The stress-strain curves of the backfill materials are shown in Fig. 3.

82 Fig. 3 shows that: (1) The stress-strain curves all had two phases: a) a rapid deformation phase up to 1 MPa, and b)
83 slower deformation thereafter, up to 6 MPa; (2) During the slow deformation phase, the stress-strain relationship was quasi-
84 linear. Obviously, Scheme 2 was the stiffest backfill material; (3) If the compaction pressure applied to the backfill material
85 was 1 MPa or greater in the preliminary stage, the deformation of the backfill material during the later period was less.

86 **4 Roadway backfill technique**

87 The principle of roadway backfill technique is shown in Fig. 4. The length of a backfilled mining roadway is usually 150 to
88 300 m, with a width of 5 to 10 m. The width of the unexploited coal pillars is usually 2 to 5 m. The equipment for backfilling
89 the driving roadway includes the mining equipment and the backfill equipment. The mining equipment consists primarily of



90 a continuous shearer, a loader, a trackless tired vehicle, etc. while the backfill equipment is primarily a material thrower, a
91 belt conveyor, etc.

92 The design of the technique for roadway backfill includes the mining process and the backfill process. The mining
93 process is implemented by the continuous shearer, the loader and the trackless tired vehicle, retreating from the headgate to
94 the tailgate, whereas the backfill material is filled backwards from the headgate to the tailgate in the backfill process. The
95 backfill materials are conveyed to an underground storage silo by a vertical feeding system, then transported to the backfill
96 roadway, and thrown at high speed into the backfill roadway by the material thrower.

97 **5 Strata movement characteristics resulting from different roadway driving and filling sequences**

98 **5.1 Numerical simulation method**

99 **5.1.1 Modelling and parameter selection**

100 Based on the roadway layout (Fig. 4), a numerical calculation model was established using FLAC^{3D} software based on
101 working face 1301 in Changxing coal mine for roadway backfill. As shown in Fig. 5, the calculation model, with a strike
102 length, inclination length, and height of 200 m, 100 m, and 35 m, respectively, was divided into 1,026,000 elements and
103 1,071,372 nodes. A uniform stress of 1.6 MPa was applied on the upper boundary with a level constraint and a vertical
104 restraint imposed on the surrounding boundaries and bottom boundary respectively. The coal and rock mass and the backfill
105 body were simulated using a Mohr-Coulomb model and an elastic model, respectively. After a throwing force of 1 MPa was
106 imposed on the backfill material by the material thrower, the stress-strain relationship of the backfill material had an
107 approximate linear distribution. The elastic modulus of Scheme 2 was determined as 14 MPa. Table 2 lists the physical and
108 mechanical parameters of the coal and rock masses.

109 **5.1.2 Simulation scheme**

110 The numerical simulation consisted of two schemes: single roadway driving and driving on multiple roadways. Specific
111 details are as follows:

112 Scheme 1: Single roadway driving was performed on the coal seam, and the strata movement characteristics were
113 simulated for roadway driving with excavation widths of 3 m, 5 m, 7 m, and 9 m respectively. Meanwhile, the zone affected
114 by the abutment stresses borne by the roadway for different widths of the driving roadway was determined.

115 Scheme 2: The driving and filling sequence for multiple-roadways was determined according to the zone affected by
116 the abutment stress around the roadway. Meanwhile, the strata movement trends during driving on multiple roadways and
117 filling were simulated for roadway widths of 3 m, 5 m, 7 m, and 9 m.



118 **5.2 Single roadway driving**

119 According to the simulation scheme for driving on a single roadway, the distribution of the abutment stresses borne by the
120 roadway (at different widths) was obtained and is shown in Fig. 6.

121 As shown in Fig. 6, increasing the roadway width increased the maximum stress and the zone affected by the abutment
122 stress on both sides of the roadway. When the width of the excavation roadway ranged from 3 m to 9 m, the zone affected by
123 abutment stress was as high as 2.5 to 3.0 times the width of the excavation roadway. If the peak value of the abutment stress
124 changed from 2.8 to 4.3 MPa, the stress concentration factor changed from 1.1 to 1.7.

125 Finally, to ensure the stability of the surrounding rock while driving on the roadway, the distance between two adjacent
126 excavation roadways must be at least 3 times longer than the width of the excavated roadway.

127 **5.3 Driving on multiple roadways**

128 Based on the simulation of driving on a single roadway, the distance between two adjacent roadways was designed to be 3
129 times longer than the width of the excavation roadway during driving. Meanwhile, coal pillars with a width of 3 m were
130 established between every second roadway. Roadway driving and filling was divided into four stages in total (see Fig. 7).

131 **5.3.1 Strata movement trends**

132 Based on the simulation scheme for driving on multiple roadways, the roof subsidence for different widths of roadway
133 driving can be obtained (Fig. 8).

134 Fig. 8 shows that: (1) Roof subsidence gradually increased with the width of the roadway. On roadways of the same
135 width, driving and filling at each stage increased the roof subsidence; (2) When the width of excavation roadway ranged
136 from 3 to 9 m, the maximum roof subsidence in the first, second, third, and fourth stages varied between 4 to 14 mm, 5 to 16
137 mm, 9 to 43 mm, and 16 to 252 mm, respectively. Additionally, roof subsidence above the coal pillar was less than that in
138 the backfill body; (3) In the first, second, and third stages, different stresses on the coal pillar and backfill body led to a
139 wave-shaped roof subsidence curve. In the fourth stage, the subsidence curve tended to be smooth after the roof was
140 stabilised.

141 In summary, the design of a roadway driving sequence and the roadway length can reduce the effects of mining
142 between two roadways. Meanwhile, the joint support of established coal pillars and the backfill body can effectively control
143 strata movement.

144 **5.3.2 Stress distribution in the mining field**

145 Fig. 9 shows the stress distribution in the mining field for different roadway widths during driving on multiple roadways.

146 The following conclusions were drawn from the results shown in Fig. 9: (1) At the same stage, the stress on the mining
147 field gradually increased with increasing roadway width. Meanwhile, for roadways of the same width, driving and filling at



148 each stage gradually increased the stress in the mining field; (2) When the width of the roadway changed from 3 to 9 m, the
149 maximum stresses in the first, second, third, and fourth stages in the mining field were between 2.8 to 3.9 MPa, 3.1 to 4.3
150 MPa, 3.8 to 5.9 MPa, and 4.3 to 7.4 MPa, respectively; (3) The overlying strata subsided with driving and filling at each
151 stage. As a result, the coal pillars were gradually compressed, and the stress borne by the coal pillars increased, reaching a
152 maximum in the middle of the mining field; (4) As the main supporting body, the backfill effectively changed the stress state
153 in the surrounding rock during the backfill process of the driving roadway. Meanwhile, the design of the roadway driving
154 sequence and the roadway length avoided the superposition of mine-induced stress bulbs, and dissipated the effects of the
155 mining.

156 5.3.3 Safety evaluation of coal pillars

157 The stability of the established coal pillars must be evaluated for roadway backfill method during mining. The safety
158 coefficient is most appropriate for consideration when designing underground coal pillars - the larger the safety coefficient,
159 the lower the failure probability of the coal pillars. The safety coefficient of a coal pillar (k) is the ratio of the average
160 compressive stress (σ_p) borne by the entire coal pillar to the compressive strength (σ_c) of the coal pillar (Peng 2008):

$$161 \quad k = \frac{\sigma_p}{\sigma_c}, \quad (1)$$

162 According to our experience in the Changxing coal mine, when the width of the established coal pillars was 3 m, the
163 safety the coefficient of the coal pillars must be 2 if the coal pillar was not to fail. The compressive strength of the coal was
164 23.1 MPa. According to the stress distribution in the mining field during driving on multiple roadways, the stress borne by a
165 coal pillar peaked when the width of the driving roadway was 9 m. Therefore, coal pillar stability was evaluated at an
166 excavation roadway width of 9 m, as shown in Fig. 8(d). At a roadway width of 9 m, the maximum stress borne by a coal
167 pillar was 7.4 MPa, and the safety coefficient of the coal pillar was 3.12. When the safety coefficient of the coal pillars was
168 greater than 2.5, the failure probability of the coal pillars was approximately equal to 0% (Peng 2008), so the coal pillars did
169 not become unstable.

170 The development of the plastic zone in the mining field when the width of excavation roadway was 9 m is shown in Fig.
171 10.

172 As shown in Fig. 10, plastic zones with thicknesses of 0.5 m were generated on both sides of the coal pillars, which
173 were supported by the backfill materials. The width of the elastic regions that developed was 2 m, accounting for 67% of the
174 coal pillar cross-section, which demonstrated that no instability was generated therein.



175 **6 Movement characteristics of strata after quadratic stabilisation when backfilling the driving roadway during** 176 **mining**

177 When backfilling mining is used to mine a coal seam, the overlying strata are disturbed inducing secondary settlement. The
178 first strata movement occurred when the original reservoir was formed. The second was primarily caused by the gradual
179 compression of the overlying strata on the backfill bodies and the coal pillars. During this process, the compressed backfill
180 bodies and coal pillars give rise to the movement of the overlying strata, finally stabilising it. The movement of the strata
181 after quadratic stabilisation during backfill mining of a driving roadway is a dynamic process. It includes the mining of coal
182 seams and backfilling the driving roadway during the mining, the compression of the backfill bodies and coal pillars, the
183 gradual subsidence of the overlying strata, and the final stabilisation of the overlying strata. The roof subsidence profiles
184 after quadratic stabilisation of the backfilled driving roadway during mining are shown for different excavation roadway
185 widths in Fig. 11.

186 The results in Fig. 11 allow the following conclusions to be drawn: (1) The roof subsidence increased with an increase
187 in the excavation roadway width after quadratic stabilization. When the width of the excavation roadway changed from 3 to
188 9 m, the maximum roof subsidence changed from 16 to 252 mm; (2) As the supporting body, the backfill body absorbed and
189 transferred the mining-induced stress. With a continuous compressing force from the overlying strata, the porosity of backfill
190 body gradually decreased, leading to better control of the stability of the overlying strata.

191 **7 Analysis of an engineering application**

192 **7.1 Layout of the mining system**

193 Considering the width of the road-header and the control of the rock surrounding the roadway, the excavation roadway at the
194 working face was designed to be 7 m wide, with 3 m wide coal pillars. Fig. 12 shows the layout used in the Changxing coal
195 mine.

196 **7.2 Optimisation of the driving and filling sequence**

197 According to the distribution of the abutment stress borne by the roadway in single roadway driving, when the width of the
198 excavation roadway was 7 m, the zone affected by the abutment stress imposed on the roadway was 18 m wide. After
199 accounting for the safety factors, we determined that the distance between two adjacent driving roadways should be 21 m.
200 The design of the roadway driving and filling sequence in the 3101 working face of the Changxing coal mine can be divided
201 into four stages:

202 Driving and filling in stage 1: by driving from the head gate to the tailgate at the working face, roadway ① was
203 produced. Afterwards, roadway ② was excavated while roadway ① was filled. As shown in Fig. 13(a), this process
204 continued until the all of the driving and filling in stage 1 were finished.



205 Driving and filling in stage 2: the coal pillar was mined, resulting in the formation of roadway I. Meanwhile, coal
206 pillars with a width of 3 m were established on both sides of roadway I. Afterwards, as shown in Fig. 13(b), driving on
207 roadway II proceeded while roadway I was filled. This process continued until the driving and filling in stage 2 was
208 finished.

209 Driving and filling in stage 3: the coal pillar on the right-hand side of roadway I was mined, resulting in the formation
210 of roadway a. Meanwhile, 3 m wide coal pillars were established on both sides of roadway a. Afterwards, as shown in Fig.
211 13(c), driving on roadway b proceeded while roadway a was filled. This process continued until the driving and filling in
212 stage 3 was finished.

213 Driving and filling in stage 4: the coal pillar on the left-hand side of roadway I was mined, resulting in the formation of
214 roadway A. Meanwhile, 3 m wide coal pillars were established on both sides of roadway A. Afterwards, as shown in Fig.
215 13(d), driving on roadway B proceeded while roadway A was filled. This process continued until the driving and filling in
216 stage 4 was finished, as shown in Fig. 13(e).

217 7.3 Application effect analysis

218 At present, the 3101 working face has been advanced for 170m. To thoroughly study rock strata movement and
219 deformation rules at Changxing coal mine, ground movement observation stations were built in corresponding position
220 above the working face. Surface movement observing proceeded from January 5, 2014 to December 5, 2014.

221 According to the analysis of the surface monitoring data, the accumulated maximum subsidence at the surface
222 monitoring point is 15mm and the maximum horizontal deformation is 0.8 mm/m. These are both controlled within Grade I
223 deformation specified by State Bureau of Coal Industry. The analysis indicated that the ground basically had no obvious
224 deformation after the implementation of the roadway backfill method at 3101 working face.

225 When the roadway backfill method was adopted in Changxing coal mine, the coal recovery ratio approached 70% and
226 the compression ratio was more than 90%. Also, the loess and aeolian sand treatment capacity reached 718,000 t/a; with a
227 large amount of solid mine wastes being used as backfill materials for filling goaf. The overlying strata of the goaf is well
228 supported to prevent strata movement and surface subsidence, thereby protecting ecological environment at the local mining
229 area. Successful application of roadway backfill method in Changxing coal mine may provide some references to other coal
230 mines in the western area for improving coal recovery while protecting the environment.

231 8 Conclusions

232 By studying the strata movement characteristics when backfilling the driving roadway during mining, we arrived at the
233 following conclusions:

234 (1) The mining rate of the room and pillar method is less than 30%. Meanwhile, the coal pillars creep over time and
235 gradually fail. During pillar failure, the roof strata become fractured and their collapse progresses upwards. The method of



236 backfilling the driving roadway during longwall mining was proposed to solve these problems. In this method, the mined out
237 area is backfilled to serve as a permanent stress bearing body that supports the overburden. The overlying strata may slowly
238 sink as a consequence, therefore it is of critical importance that strata movement and surface subsidence are effectively
239 controlled.

240 (2) Aeolian sand, loess, and cementing materials were used to prepare the backfill materials in this study. Testing
241 determined the mechanical properties and compositions of the backfill materials.

242 (3) The strata movement characteristics when driving on a single roadway were obtained, and the zone affected by
243 abutment stress in the mining field was determined by simulation and used to optimise the sequence of driving on multiple
244 roadways accompanied by the acquisition of the strata movement characteristics when driving on multiple roadways.

245 (4) Roadway backfill technique during longwall mining of the 3101 working face of the Changxing coal mine was used
246 as an engineering case study in this work. Based on the strata movement characteristics of driving on single and multiple
247 roadways, the driving and filling sequence of the 3101 working face was optimised to avoid the added effects of mining-
248 induced stresses.

249 (5) According to the analysis of the surface monitoring data, the accumulated maximum subsidence is 15mm and the
250 maximum horizontal deformation is 0.8 mm/m, which indicated that the ground basically had no obvious deformation after
251 the implementation of the roadway backfill method at 3101 working face. Also the coal recovery ratio approached 70% and
252 the compression ratio was more than 90%.

253 **Acknowledgments**

254 This research was supported by the Qing Lan project (Education Department of Jiangsu) (2014(23)), Foundation for
255 Distinguished professor of Jiangsu Province (Education Department of Jiangsu) (2015(29)), and National Key Basic
256 Research Program of China (2013CB227905).

257 **Conflict of Interests**

258 The authors declare that there is no conflict of interests regarding the publication of this paper.

259 **References**

- 260 Bell, F. G., and Bruyn, I. A.: Subsidence problems due to abandoned pillar workings in coal seams, *Bull. Eng. Geol. Env.*, 57,
261 225-237, doi:10.1007/s100640050040, 1999.
- 262 Castellanza, R., Gerolymatou, E., and Nova, R.: An attempt to predict the failure time of abandoned mine pillars, *Rock Mech.*
263 *Rock Eng.*, 41, 377-401, doi:10.1007/s00603-007-0142-y, 2008.



- 264 Castellanza, R., Nova, R., and Orlandi, G.: Flooded gypsum mine remedial by chamber filling, *J. Geotech. Geoenviron. Eng.*,
265 136, 629-639, doi:10.1061/ASCE GT.1943-5606.0000249, 2010.
- 266 Chen, S. J., Guo, W. J., Zhou, H., and Wen, G. H.: Structure model and movement law of overburden during strip pillar
267 mining backfill with cream-body, *J. China Coal Soc.*, 36, 1081-1086, 2011. (in Chinese, with English Abstract.)
- 268 Chen, S. J., Zhou, H., Guo, W. J., Wang, H.L., and Sun, X. Z.: Study on long-term stress and deformation characteristics of
269 strip pillar, *J. Min. Safety. Eng.*, 29, 376-380, 2012. (in Chinese, with English Abstract.)
- 270 Cui, X. M., Gao, Y. G., and Yuan, D. B.: Sudden surface collapse disasters caused by shallow partial mining in Datong
271 coalfield, China, *Nat. Hazards*, 74, 911-929, doi:10.1007/s11069-014-1221-5, 2014.
- 272 Ding, H. D., Miao, X. X., Ju, F., Wang, X. L., and Wang, Q. C.: Strata behavior investigation for high-intensity mining in
273 the water-rich coal seam, *Int. J. Min. Sci. Tech.*, 24, 299-304, doi:10.1016/j.ijmst.2014.03.002, 2014.
- 274 Ghasemi, E., Ataei, M., Shahriar, K., Sereshki, F., Jalali S. E., and Ramazanzadeh, A.: Assessment of roof fall risk during
275 retreat mining in room and pillar coal mines, *Int. J. Rock Meh. Min. Sci.*, 54, 80-89, doi:10.1016/j.ijrmms.2012.05.025, 2012.
- 276 Gutierrez, F., Parise, M., Waele, J. D., and Jourde, H.: A review on natural and human-induced geohazards and impacts in
277 karst, *Earth Sci. Rev.*, 138, 61-88, doi:10.1016/j.earscirev.2014.08.002, 2014.
- 278 Guo, L. Q., Cai, Q. P., and Peng, X.Q.: Effect of strength criterion on design of strip coal pillar, *Rock Soil Mech.*, 35, 777-
279 782, 2014a. (in Chinese, with English Abstract.)
- 280 Guo, G. L., Zhu, X. J., Zha, J. F., and Wang, Q.: Subsidence prediction method based on equivalent mining height theory for
281 solid backfilling mining, *T. Nonferr. Metal. Soc. China*, 24, 3302-3308, doi:10.1016/S1003-6326(14)63470-1, 2014b.
- 282 Junker, M., and Witthaus, H.: Progress in the research and application of coal mining with stowing, *Int. J. Min. Sci. Tech.*,
283 23, 7-12, doi:10.1016/j.ijmst.2013.01.002, 2013.
- 284 Kostecki, T., and Spearing, A. J. S.: Influence of backfill on coal pillar strength and floor bearing capacity in weak floor
285 conditions in the Illinois Basin, *Int. J. Rock. Mech. Min. Sci.*, 76, 55-67, doi:10.1016/j.ijrmms.2014.11.011, 2015.
- 286 Lollino, P., Martimucci, V., and Parise, M.: Geological survey and numerical modeling of the potential failure mechanisms
287 of underground caves, *Geosy. Eng.*, 16, 100-112, doi:10.1080/12269328.2013.780721, 2013.
- 288 Li, M., Zhang, J. X., and Miao, X. X.: Experimental investigation on compaction properties of solid backfill materials, *Min.*
289 *Tech.*, 123, 193-198, doi:10.1179/1743286314Y.0000000066, 2014.
- 290 Peng, S. S.: *Coal mine ground control*, 3rd edn. Peng SS publisher, Morgantown, WV, 2008.
- 291 Parise, M., and Lollino, P.: A preliminary analysis of failure mechanisms in karst and man-made underground caves in
292 Southern Italy, *Geomorphology*, 134, 132-143, doi:10.1016/j.geomorph.2011.06.008, 2011.
- 293 Parise, M.: A present risk from past activities: sinkhole occurrence above underground quarries, *Carbonates and Evaporites*,
294 27, 109-118, doi:10.1007/s13146-012-0088-3, 2012.
- 295 Parise, M.: Karst geo-hazards: causal factors and management issues, *Acta Carsologica*, 44, 401-414,
296 doi:10.3986/ac.v44i3.1891, 2015.
- 297



- 298 Pasten, D., Estay, R., Comte, D., and Vallejos, J.: Multifractal analysis in mining microseismicity and its application to
299 seismic hazard in mine, *Int. J. Rock Mech. Min. Sci.*, 78, 74-78, doi:10.1016/j.ijrmms.2015.04.020, 2015.
- 300 Shi, L. Q., and Singh, R. N., Study of mine water inrush from floor strata through faults, *Mine Water Environ.*, 20, 140-147,
301 doi:10.1007/s10230-001-8095-y, 2001.
- 302 Si, H., Bi, H. P., Li, X. H., and Yang, C. H.: Environmental evaluation for sustainable development of coal mining in Qijiang,
303 Western China, *J. Coal Geol.*, 81, 163-168, doi:10.1016/j.coal.2009.11.004, 2010.
- 304 Sun, X. K., and Wang, W.: Theoretical research on high water material replacement mining the strip coal pillar above
305 confined aquifer, *J. China Coal Soc.*, 36, 909-913, 2011. (in Chinese, with English Abstract.)
- 306 White, W. B.: Karst hydrology: recent developments and open questions, *Eng. Geol.*, 65, 85-105, doi:10.1016/S0013-
307 7952(01)00116-8, 2002.
- 308 Wu, Q., Zhou, W. F., Li, D., Di, Z. Q., and Miao, Y.: Management of karst water resources in mining area: dewatering in
309 mines and demand for water supply in the Dongshan Mine of Taiyuan, Shanxi Province, North China, *Environ. Geol.*, 50,
310 1107-1117, doi:10.1007/s00254-006-0284-3, 2006.
- 311 Wang, X. F., Zhang, D. S., Zhang, W., and Xu, M. T.: Support resistance determination for shallow coal seam longwall
312 mining in sand-soil gullies overlaying mining area, *J. China Coal Soc.*, 38, 194-198, 2013. (in Chinese, with English
313 Abstract.)
- 314 Xie, X. Z.: Study on the characteristics of strata behavior in shallow seam longwall mining under the room-and-pillar mining
315 goaf, *J. China Coal Soc.*, 37, 898-302, 2012. (in Chinese, with English Abstract.)
- 316 Yu, W. J., and Wang, W. J.: Strata movement induced by coal-pillar under three circumstances exchanged by gangue
317 backfill and quadratic stability law, *Chinese J. Rock Mech. Eng.*, 30, 105-112, 2011. (in Chinese, with English Abstract.)
- 318 Zhang, J. X., Miao, X.X., Mao, X.B., and Chen, Z.W.: Research on waste substitution extraction of strip extraction coal-
319 pillar mining, *Chinese J. Rock Mech. Eng.*, 26, 2687-2693, 2007. (in Chinese, with English Abstract.)
- 320 Zhang, J. X., Zhou, N., Huang, Y. L., and Zhang, Q.: Impact law of the bulk ratio of backfilling body to overlying strata
321 movement in fully mechanized backfilling mining. *J. Min. Sci.*, 47, 73-84, doi:10.1134/S1062739147010096, 2011.
- 322 Zhai, C., Xiang, X. W., Xu, J. Z., and Wu, S. L.: The characteristics and main influencing factors affecting coal and gas
323 outbursts in Chinese Pingdingshan mining region, *Nat. Hazards*, 82, 507-530, doi:10.1007/s11069-016-2195-2, 2016.



325 **Tables and Figures:**

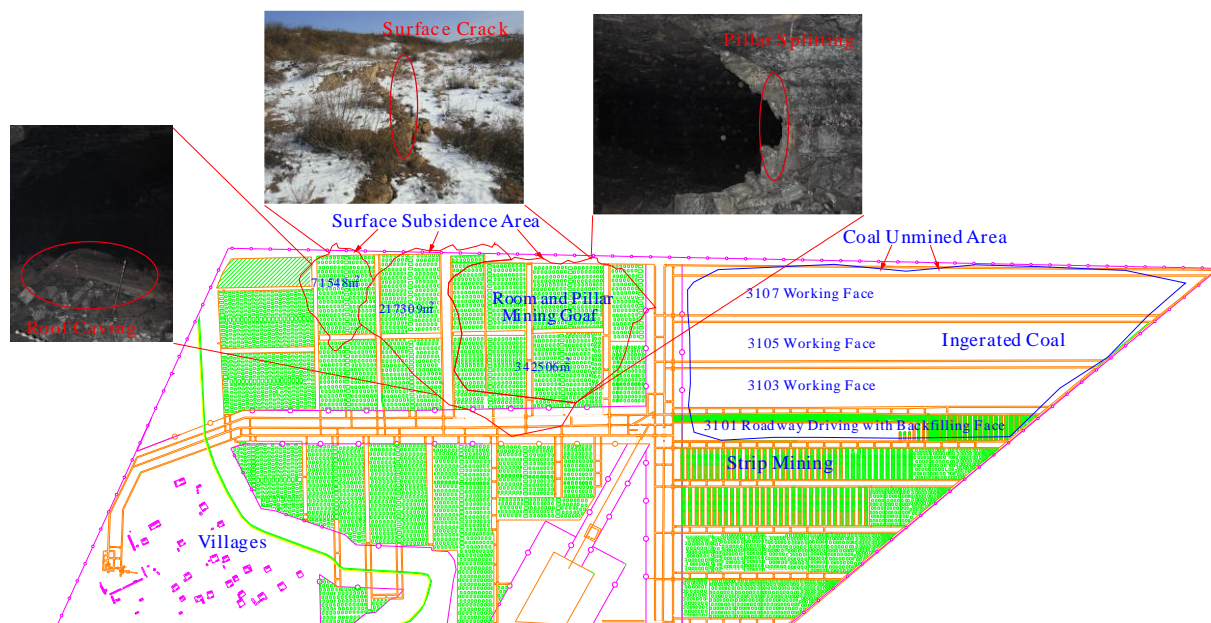
326 **Table 1.** Composition of backfill materials (percent by weight).

Sample No.	Aeolian sand	Ratio of loess	Cementing material
1	70	20	10
2	68	20	12
3	67	20	13
4	61	30	9
5	60	30	10
6	58	30	12
7	51	40	9
8	50	40	10
9	48	40	12

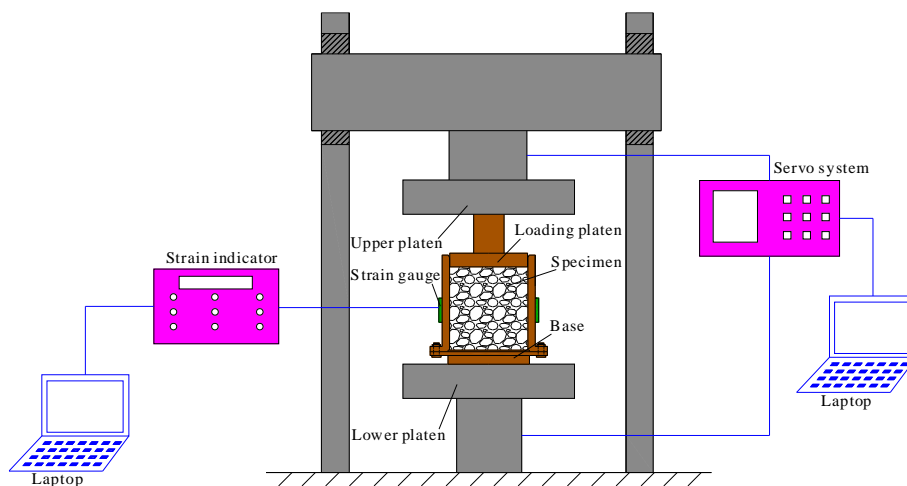
327

328 **Table 2.** Physico-mechanical parameters of the coal and rock mass.

Rock layer	Thickness (m)	Bulk modulus (GPa)	Tensile strength (MPa)	Cohesion (MPa)	Friction angle (°)	Density (kg/m ³)
Main roof	11.6	1.5	2.8	32	32	2200
Immediate roof	4.5	0.8	1.6	28	28	1600
Coal seam	5.35	0.6	1.2	21	21	1400
Floor	7.6	1.0	1.8	28	28	1600

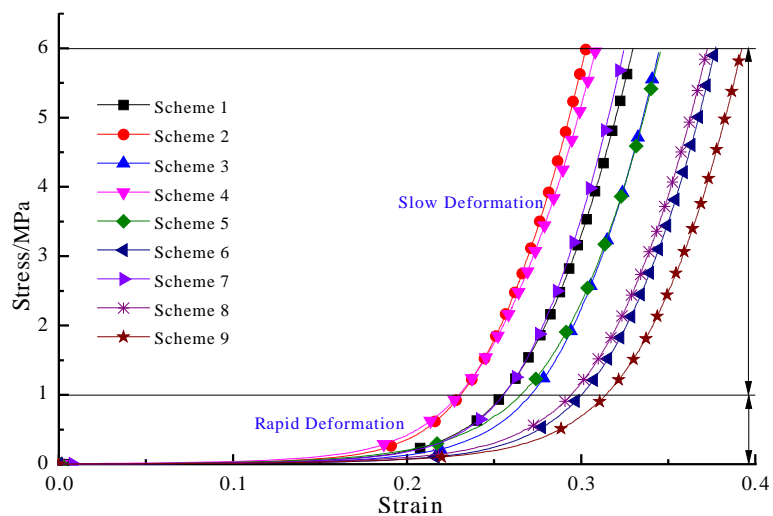


329
330 **Figure 1.** Surface subsidence induced by room and pillar mining in Changxing coal mine.



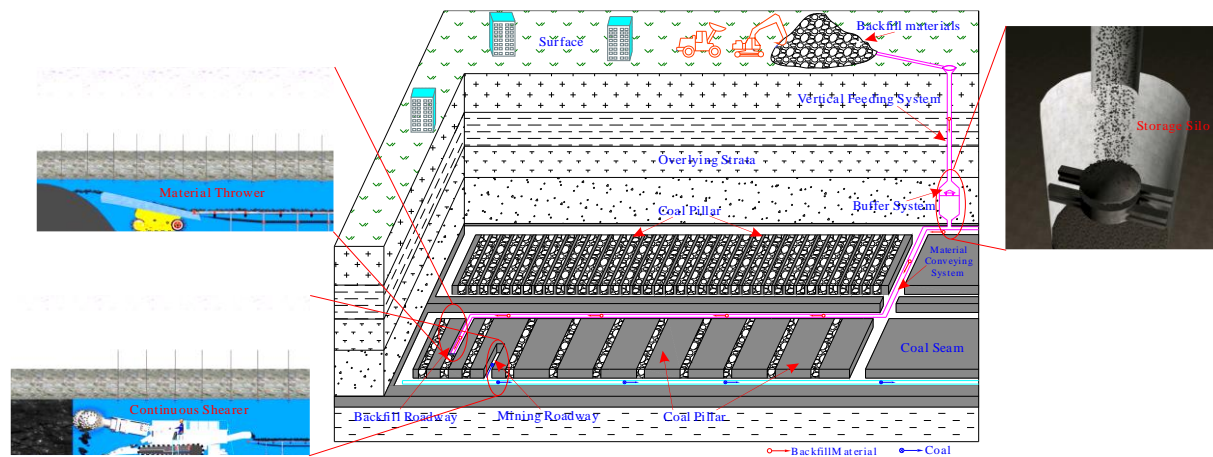
331
332

Figure 2. Schematic diagram of test system.



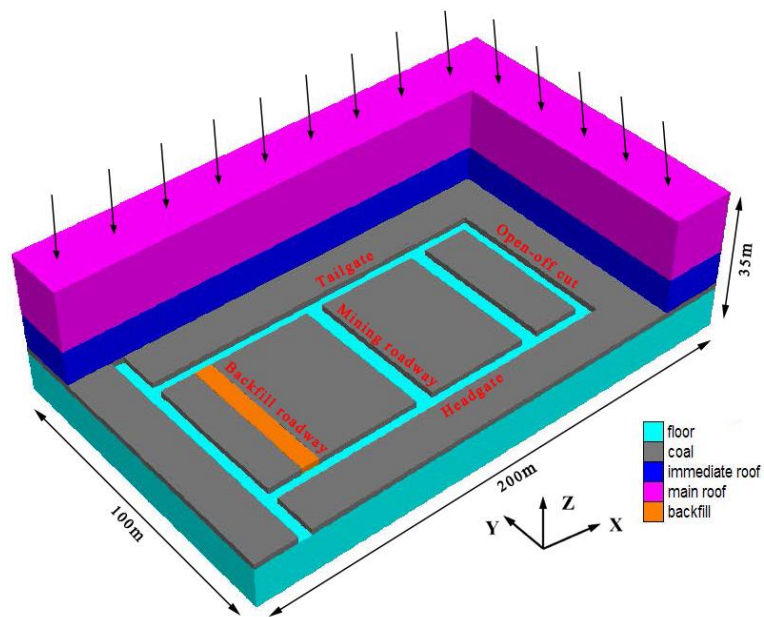
333

334 **Figure 3.** Stress-strain curves of backfill materials.



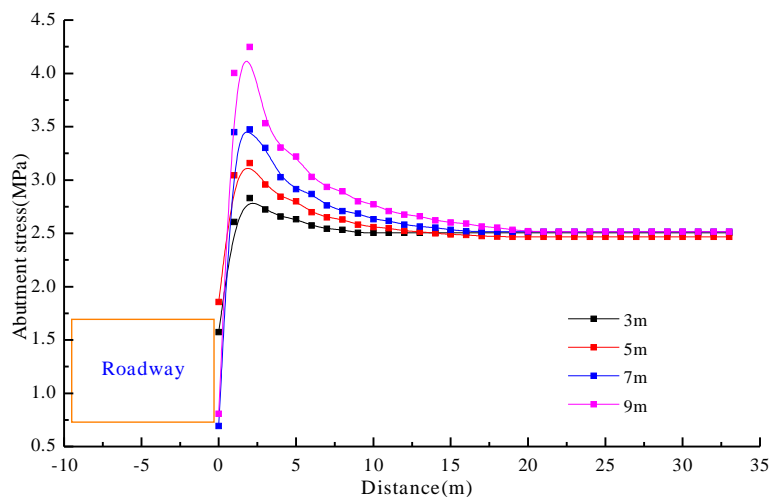
335

336 **Figure 4.** Principle of roadway driving with backfill technique.



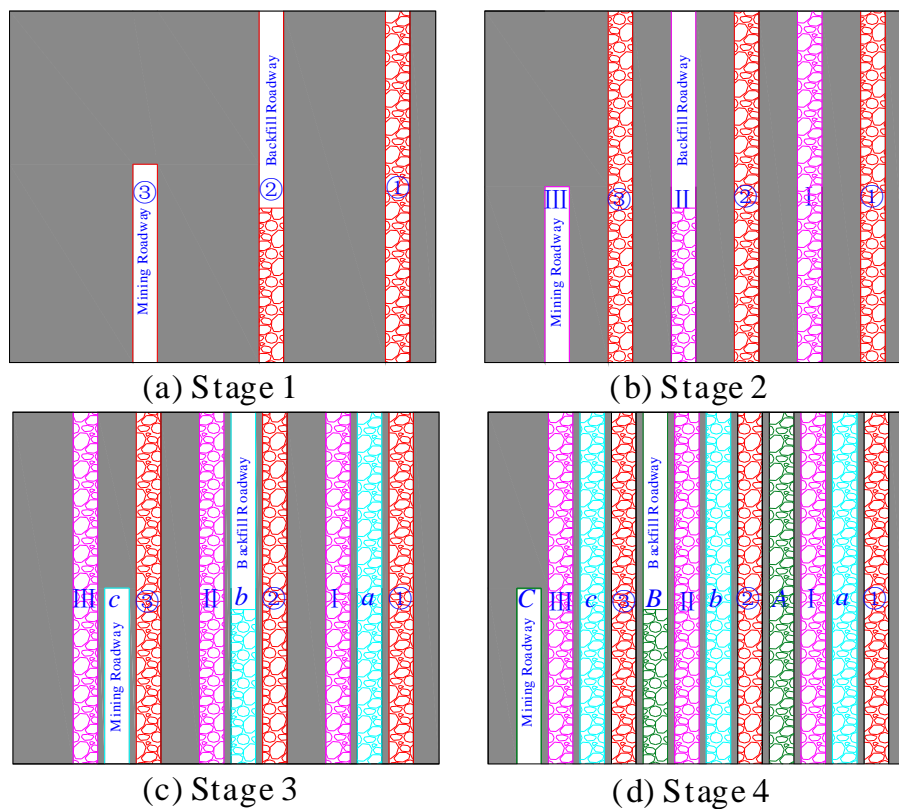
337

338 **Figure 5.** Numerical calculation model.

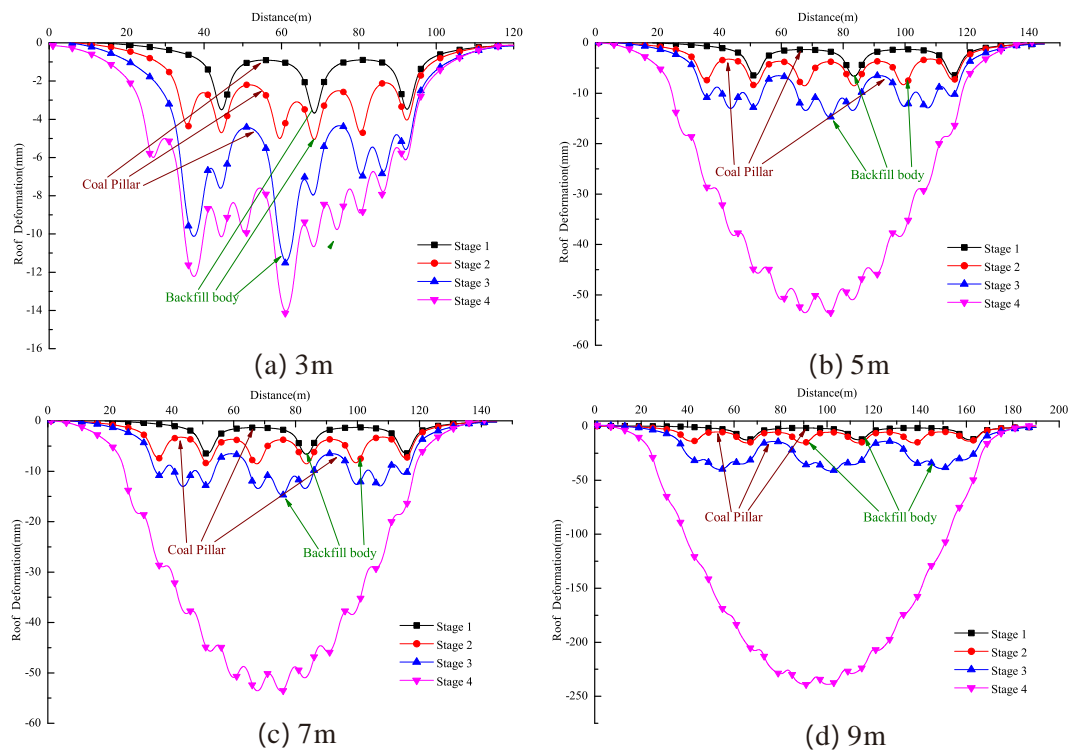


339

340 **Figure 6.** Distribution of abutment stresses on the roadway.

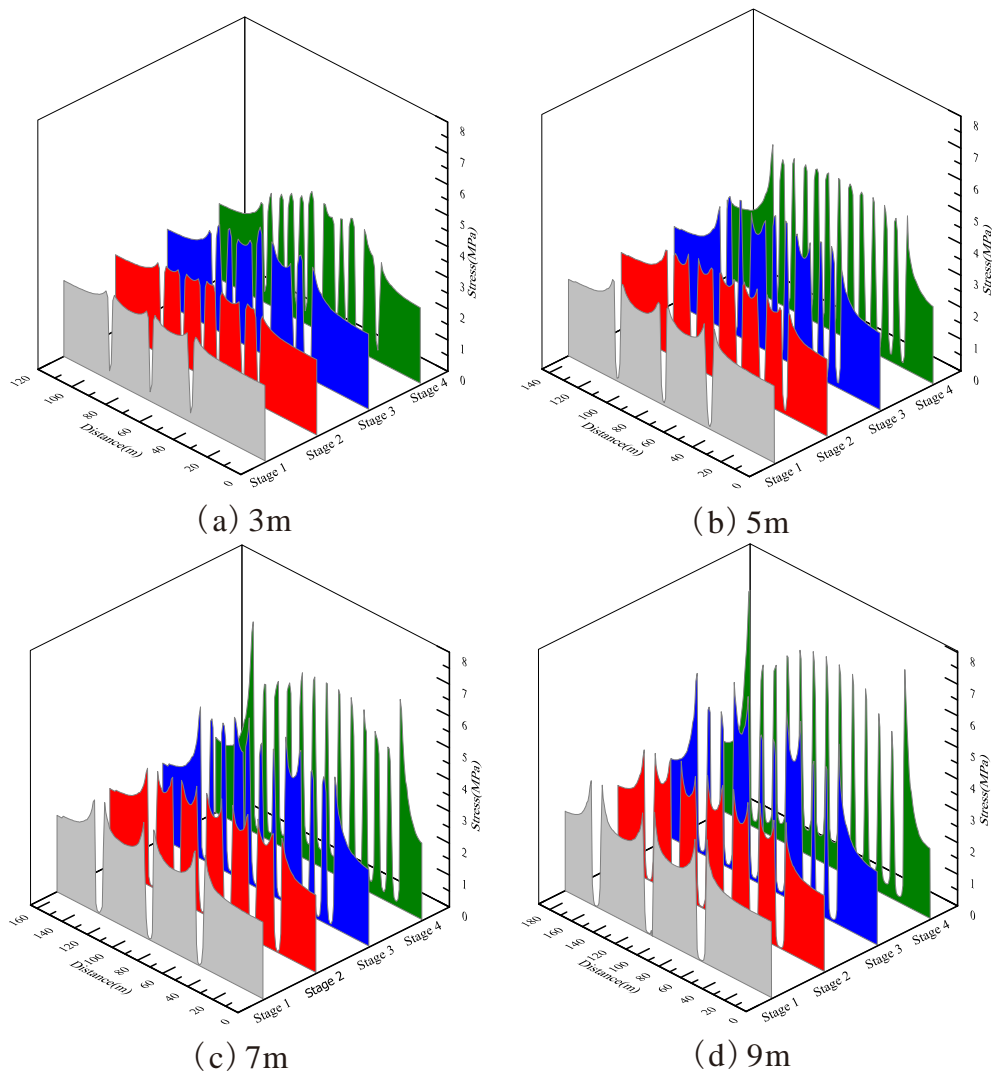


341
 342 **Figure 7.** Simulation of driving on multiple roadways.

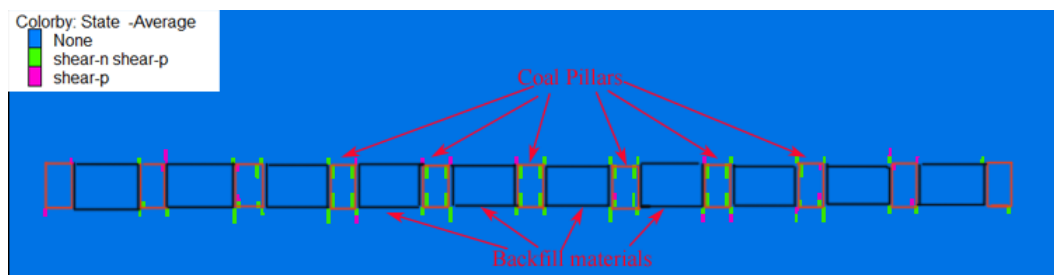


343

344 **Figure 8.** Roof subsidence with different width of roadway.

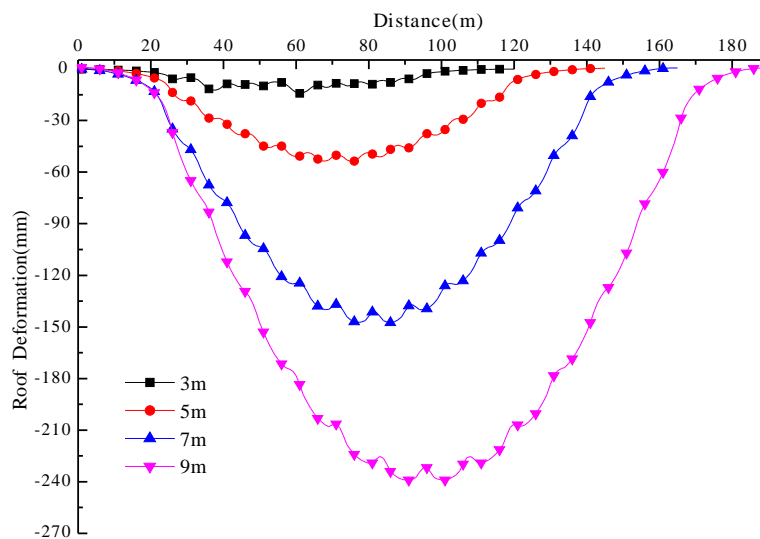


345
346 **Figure 9.** Stress distributions with different width of roadway.



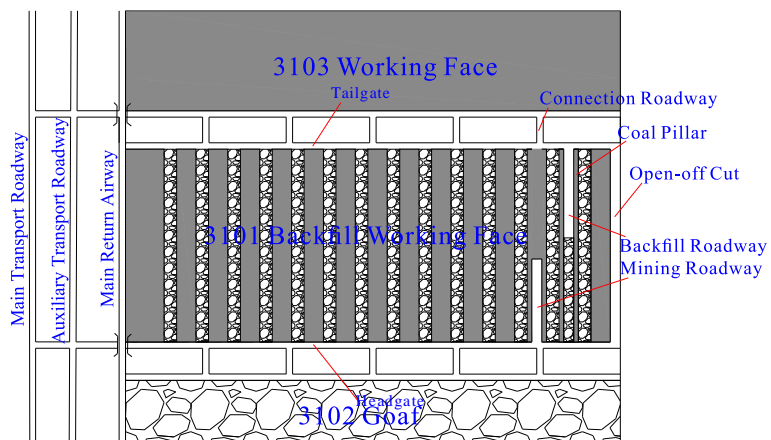
347

348 **Figure 10.** The plastic zone distribution for a 9 m wide excavation roadway.



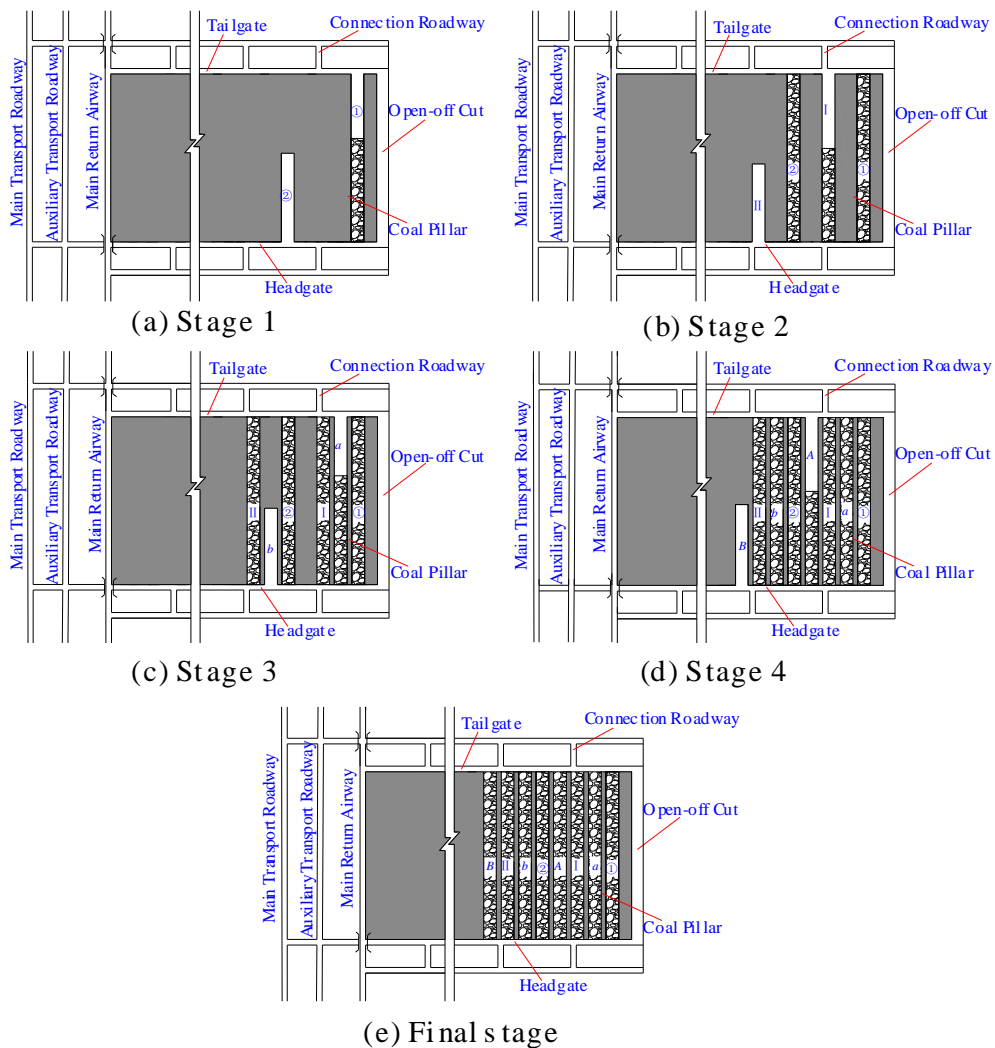
349

350 **Figure 11.** Roof subsidence after quadratic stabilisation.



351

352 **Figure 12.** Layout of the mining system used in the Changxing coal mine.



353

354 Figure 13. Design of the driving and filling sequence in the backfill of the driving roadway during mining.